

Microscopic theory for a ferromagnetic-nanowire/superconductor heterostructure: Transport, fluctuations and topological superconductivity

So Takei¹ and Victor Galitski^{1,2,3}

¹*Condensed Matter Theory Center, The Department of Physics,
The University of Maryland, College Park, MD 20742-4111, USA*

²*Joint Quantum Institute, The University of Maryland, College Park, MD 20742-4111, USA*

³*Kavli Institute for Theoretical Physics, University of California Santa Barbara, CA 93106-4030*

(Dated: November 3, 2018)

Motivated by the recent experiment of Wang *et al.* [Nature Physics **6**, 389 (2010)], who observed a highly unusual transport behavior of ferromagnetic Cobalt nanowires proximity-coupled to superconducting electrodes, we study proximity effect and temperature-dependent transport in such a mesoscopic hybrid structure. It is assumed that the asymmetry in the tunneling barrier gives rise to the Rashba spin-orbit-coupling in the barrier that enables induced p -wave superconductivity in the ferromagnet to exist. We first develop a microscopic theory of Andreev scattering at the spin-orbit-coupled interface, derive a set of self-consistent boundary conditions, and find an expression for the p -wave minigap in terms of the microscopic parameters of the contact. Second, we study temperature-dependence of the resistance near the superconducting transition and find that it should generally feature a fluctuation-induced peak. The upturn in resistance is related to the suppression of the single-particle density of states due to the formation of fluctuating pairs, whose tunneling is suppressed. In conclusion, we discuss this and related setups involving ferromagnetic nanowires in the context of one-dimensional topological superconductors. It is argued that to realize unpaired end Majorana modes, one does not necessarily need a half-metallic state, but a partial spin polarization may suffice. Finally, we propose yet another related class of material systems – ferromagnetic semiconductor wires coupled to ferromagnetic superconductors – where direct realization of Kitaev-Majorana model should be especially straightforward.

PACS numbers: 74.40.+k, 74.81.Bd, 64.60.Ak

I. INTRODUCTION

Coexistence of ferromagnetism and superconductivity is a rare phenomenon, yet there exists unambiguous evidence for its occurrence. Superconductivity has been thoroughly investigated in the uranium-based itinerant ferromagnets^{1–4} and there have been reports about possible co-existence of these phases in the d -electron compound ZrZn_2 ⁵ and the copper oxide compound $\text{RuSr}_2\text{GdCu}_2\text{O}_{8-\delta}$ (Ru-1212)^{6–9}. The neutron diffraction measurements in ferromagnetic superconductors ErRh_4B_4 ¹⁰, HoMo_6S_8 ¹¹ and HoMo_6Se_8 ¹² indicate an inhomogeneous magnetic order coexisting with superconductivity. More recently, coexistence of these seemingly exclusive states was also seen in Pb/PbO core/shell nanoparticles¹³, and in two-dimensional interfaces between perovskite band insulators LaAlO_3 and SrTiO_3 ^{14,15}.

The interplay of superconductivity and ferromagnetism can also be studied in the context of superconducting proximity effect, where a superconductor in contact with a normal metal induces superconducting correlations in the latter. Due to incompatible spin order conventional superconducting correlations are known to penetrate negligibly inside a ferromagnet.¹⁶ However, a number of recent studies have demonstrated an unexpectedly long-ranged proximity effect in mesoscopic superconductor-ferromagnet hybrid structures.^{17–22} A subsequent theoretical work showed that local inhomogeneity in the magnetization near the interface can induce triplet-pairing inside the ferromagnet, and that these correlations can account for the observed long-ranged proximity effect.²³ This beautiful theory predicts an exotic odd-frequency (even-momentum) symmetry for the triplet component of the condensate, which was originally suggested by Berenzinskii as a possible phase in superfluid ^3He .²⁴ Theoretical work on the Josephson coupling between two conventional superconductors separated by a half-metallic ferromagnet has also investigated the mechanism behind singlet-to-triplet conversion near a half-metal-superconductor interface.^{25,26}

Seemingly unrelated to the developments in superconducting proximity effect at the time, Kitaev showed in his pioneering work that Majorana fermion excitations can be localized at the ends of a spinless $p_x + ip_y$ superconducting quantum wire.²⁷ Conceptually, the Kitaev model of a topological superconductor is that of a fully-polarized ferromagnetic superconductor. However, a direct connection between the model and the existing ferromagnetic itinerant and hybrid superconducting systems has been made only very recently. In some of the recent proposals, superconducting proximity effect plays a key role in realizing topological superconductors which support Majorana fermions on their boundaries or in a vortex core.^{28–40}

On the experimental front, Ref. 21 has already shown that a ferromagnetic cobalt (Co) quantum wire can be made superconducting by placing it in contact with a

conventional superconductor. Proximity-induced superconductivity was observed in the wire over a distance of a few hundred nanometers. The pairing symmetry inside the wire is likely to be a spin-triplet state since singlet correlations should not survive inside the ferromagnet over a distance exceeding a few nanometers. While the odd-frequency superconductivity indeed remains a viable explanation of the long-range proximity effect, an alternative scenario in clean wires involves p -wave superconductivity induced by a spin-orbit coupled interface.³⁵ The latter would imply that an experiment of the kind in Ref. 21 is very close to realizing the topological superconductor²⁷, and may host the sought-after Majorana fermions at the two ends of the wire or inside the wire, wherever the parity of the number of occupied sub-bands changes.

With its broader physical relevance aside, the experimental work of Ref. 21 has made very interesting observations in the context of superconducting proximity effect in ferromagnetic systems. The work systematically studies the resistance of ferromagnetic single-crystal cobalt nanowires sandwiched between two superconducting electrodes. They observe proximity-induced superconductivity in the nanowire over a distance of order 500nm, which is orders of magnitude longer than the coherence length expected for conventional superconducting correlations inside a ferromagnet. For some wires, transition to superconductivity is preempted by a large and sharp resistance peak near the transition temperature of the electrodes. The resistance peak disappears when the Co wire is replaced by a gold wire, indicating an intimate connection between it and the ferromagnetism of the wire.

Motivated by these observations, we first theoretically study the physics of an s -wave-superconductor-ferromagnet tunnel junction. We assume that the asymmetry in the tunneling barrier gives rise to the Rashba spin-orbit coupling inside the tunnel barrier and enables p -wave superconductivity to be induced inside the ferromagnet.³⁵ We derive a complete set of relevant boundary conditions, and an expression for the p -wave minigap is found in terms of the microscopic parameters of the contact. In the second part of the work, we investigate in detail how the anomalous resistance peak can be explained based on the theory of superconducting fluctuation corrections to conductivity.^{41,42} We discuss a possible faithful model for the cobalt nanowire in the vicinity of the deposited W electrodes, develop a microscopic theory for the superconducting fluctuations in the W electrodes, and study how these fluctuations influence the resistance of the cobalt wire. Finally, we discuss in more detail the possible relevance of the experiment to topological superconductivity and propose a related hybrid system, which provides in our opinion the simplest physical realization of topological superconductivity and localized Majorana modes.

We emphasize that the Co wire throughout the work is treated mostly in the ballistic/ballistic-to-diffusive crossover limit. As we outline in later parts of the paper,

the treatment of the wire in this limit is reasonably justified based on experimental data²¹ and past studies on Co band structure^{43–46}, although the information available to us is insufficient to conclusively determine the nature of proximity-induced superconductivity in the hybrid system. As we have mentioned above, long-ranged *odd-frequency* p -wave proximity effect, extensively studied in diffusive ferromagnets^{22,23}, remains another realistic scenario. Here, we are exploring the possibility of a long-ranged *spatially-odd* p -wave proximity effect induced via interfacial spin-orbit coupling, which remains a viable physical scenario when the ferromagnet is in the clean limit. Furthermore, as argued below, this latter mechanism may survive even in disordered systems due to mesoscopic fluctuation effects.

The paper is organized as follows. Sec. II summarizes the main findings of the experiment in Ref. 21, with a particular emphasis on the critical resistance peak. The section also lays out in detail an estimate for the mean-free path of the Co wire and a justification for considering the clean limit. A microscopic theory for Andreev scattering at a ferromagnet-superconductor interface is presented in Sec. III. In Sec. IV, the superconducting fluctuation theory is applied to the W electrodes. Following a qualitative discussion on how superconducting fluctuations in the W can lead to resistance peaks in Co transport, a detailed microscopic theory for the corrections to resistance from these fluctuations is developed in Sec. IV A. A discussion of topological superconductivity is presented in Sec. V.

II. SUMMARY OF THE PENN STATE EXPERIMENT

Ref. 21 reports observations of long-ranged proximity effect in single-crystal ferromagnetic Co nanowires. Resistance of the wire is studied using a four-probe setup with all four electrodes made from superconducting tungsten (W) [see Fig. 1(a)] or with a combination of superconducting W and non-superconducting platinum (Pt) electrodes [see Fig. 1(b)]. While the outer electrodes are used to pass current i_w through the wire, the inner electrodes are used to measure the potential difference across a length L of the wire. With superconducting voltage electrodes [Fig. 1(a)] Co wires become fully superconducting below the electrode transition temperature for $L = 600\text{nm}$, and show substantial resistance drop for $L = 1.5\mu\text{m}$. However, such resistance drop was not observed when the superconducting electrodes are replaced by non-superconducting Pt. However, when an additional electrically isolated W strip is deposited between the Pt electrodes (see Fig. 1(c)), proximity-induced superconducting properties are restored in the Co wire.

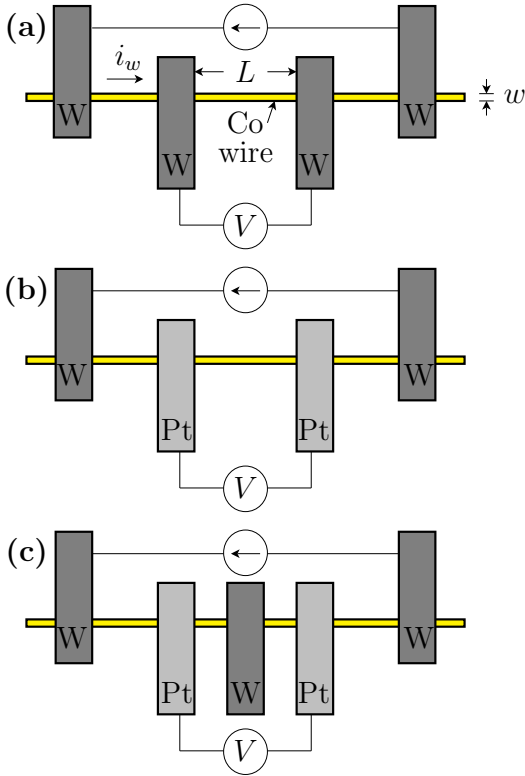


FIG. 1: A cartoon representation of the various experimental setups used in Ref. 21. Three main setups are considered: (a) W current and voltage electrodes; (b) W current electrodes and Pt voltage electrodes; and (c) same as (b) with an additional electrically isolated W strip between the Pt electrodes. Length of the wire L is determined by the distance between the inner edges of the voltage electrodes. The width (or diameter) of the Co wire is denoted by w .

A. Critical resistance peak

The most interesting observation in the experiment is that the resistance shows a sharp peak as a function of temperature as it approaches the superconducting transition temperature of the W electrodes. A cartoon picture of a typical resistance versus temperature curve is shown in Fig. 2 to illustrate this result. The transition temperature of the electrodes is estimated to be between $T_c = 4.4\text{-}5\text{K}$. This resistance peak is very large and constitutes 25-100% of the normal state resistance depending on the wire width. Intriguingly, the peak disappears when the Co wire is replaced by a paramagnetic gold wire, and thus seems to be a consequence of the ferromagnetism of the Co wire. The large resistance peak also disappears when the W electrodes are replaced by Pt electrodes [see Fig. 1(b)], but is restored once an electrically isolated W strip is deposited [see Fig. 1(c)]. The large resistance upturn thus seems to require only that a superconducting strip is in contact with the nanowire, and does not require it to be either a current or a voltage electrode.

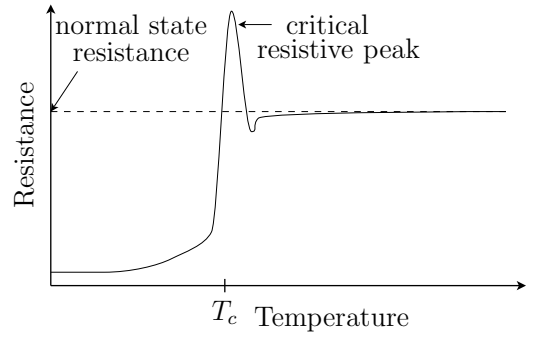


FIG. 2: A cartoon plot of the experimentally observed Co wire resistance as a function of temperature. A critical resistance peak is observed near the transition temperature T_c of the W electrodes. A precipitous drop in the resistance is then observed below T_c .

B. Mean-free path

When the extra W strip is deposited on the wire [see Fig. 1(c)] data show that the wire's normal state resistance increases by approximately 55Ω . This amounts to a nearly 50% increase from its normal state resistance of $\approx 126\Omega$ prior to the deposition [see Fig. 1(b)]. This suggests that the deposition process could have strongly modified the property of the wire in the vicinity of the contact. Returning to the setup in Fig. 1(a) the experimental data show total normal state wire resistance of approximately 145Ω . The resistance of the Co wire arising from regions unaffected by the W strips can then be approximated as $145\Omega - 2 \cdot 55\Omega = 35\Omega$. Using the quoted distance between the voltage electrodes (i.e. $L = 1.5\mu\text{m}$) and the wire width (i.e. $w = 36\text{nm}$) the corresponding resistivity is $\rho \approx 23\text{n}\Omega\cdot\text{m}$. An estimate for Co's Fermi velocity, based on critical current oscillations observed in a Nb/Co/Nb Josephson junction, gives $v_F \approx 280\text{km/s}$.⁴⁷ From this the density for electrons with a single spin projection can be estimated as

$$n = x^3 \frac{m_e^3 v_F^3}{6\pi^2 \hbar^3} \approx x^3 \cdot 2.4 \times 10^{26} \text{m}^{-3}, \quad (1)$$

where $x = m^*/m_e$ is the Co effective mass ratio with m^* being the effective mass of the Co electrons and m_e the mass of the electron. The Drude formula then gives a mean-free path estimate of

$$\ell = \frac{x m_e v_F}{n e^2 \rho} \approx \frac{1.8\mu\text{m}}{x^2}. \quad (2)$$

Cores of the Co nanowires studied in Ref. 21 show a hexagonal close-packed zone pattern and the wires have a [0001] growth direction. Presumably, the electron transport through the wire is then along the c -axis direction.

For our estimate of the Co effective mass x , we use results based on band structure calculations for Co cyclotron mass.⁴⁶ In the relevant direction of transport, we have $x \approx 3$. Inserting this value into (2) the mean-free path is estimated to be $\ell \approx 200\text{nm}$, which is the same order of magnitude as the observed coherence length in the Co wire. Within this scenario, regions of the Co wire unaffected by the W electrodes can be considered in the clean limit.

We note, however, that the above estimate for the mean-free path relies crucially on our estimate for the resistance of the Co wire unaffected by the W electrodes. Furthermore, the estimate also depends sensitively on the values used for v_F and x , which we do not know with certainty. Due to Co's complicated band structure, the values for v_F and x strongly depend on the direction of transport with respect to the crystallographic axes and on the Fermi surface which gives the dominant contribution to transport. For instance, for $v_F \sim 10^6\text{m/s}$ (quoted in Ref. 21) we obtain a much shorter mean-free path of $\ell \approx 16\text{nm}$, implying that the wire is in the diffusive limit. Co having multiple subbands with varying x also implies that some subbands are less affected by disorder than others. If all bands participating in transport indeed have short mean-free paths (of order a few nanometers), the likely mechanism for proximity effect is the spatially even, odd-frequency pairing.^{22,23} However, based on experimental data in Ref. 21 and on Co band structure and de-Haas-van Alphen studies relevant for electron transport in the c -axis direction⁴⁶, we have shown above that there is reasonable justification to model the Co wire in the clean limit, and the spatially odd p -wave pairing is a viable mechanism for the observed proximity effect. Furthermore, mesoscopic fluctuation effects may further enable remnants of p -wave superconductivity to persist well into the diffusive limit.⁴⁸ In this work, we pursue this scenario of a Co wire with proximity-induced p -wave superconductivity, and purport that it provides a natural explanation for the resistance peak.

III. ANDREEV REFLECTION AT A FM-SC INTERFACE

We consider a tunnel junction consisting of a ferromagnetic normal metal at $0 \leq z < d$, a tunneling barrier at $-a < z < 0$, and a superconductor at $z \leq -a$ (see Fig. 3). At the moment, we assume translational symmetry in the direction(s) parallel to the interfaces. We will work with a planar junction, but the results will also describe proximity effect in a ferromagnetic nanowire by simply “removing” one of the two transverse directions or by choosing a specific transverse sub-band. The derivation below follows closely that of Refs. 49 and 50, but is generalized to include spin-orbit-coupling effects in the barrier.

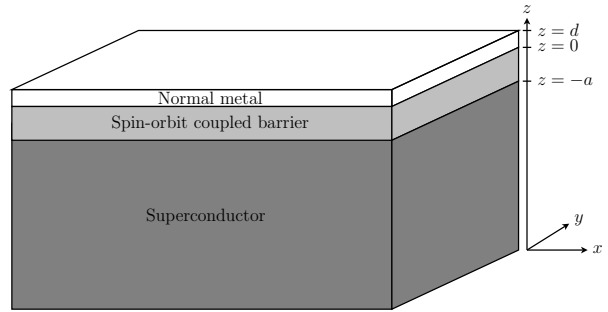


FIG. 3: The proximity tunnel junction considered. The ferromagnetic normal metal, the tunnel barrier with spin-orbit coupling and the superconductor occupy $0 \leq z < d$, $-a < z < 0$ and $z \leq -a$, respectively.

A. Equations of motion

The electron field operators in the ferromagnet $\psi^{(F)}$, tunnel barrier $\psi^{(B)}$ and superconductor $\psi^{(S)}$ satisfy the following equations of motion. In the normal region ($0 \leq z < d$),

$$\left[\left(\varepsilon - \xi_{\mathbf{p}}^{(F)} + \frac{\hbar^2 \partial_z^2}{2m_F} \right) \delta_{\alpha\beta} - (\mathbf{h} \cdot \boldsymbol{\sigma}_{\alpha\beta}) \right] \psi_{\beta, \mathbf{p}}^{(F)}(z) = 0; \quad (3)$$

in the barrier ($-a < z < 0$),

$$\left[\left(\varepsilon - U_0 - \frac{\mathbf{p}^2 - \hbar^2 \partial_z^2}{2m_B} \right) \delta_{\alpha\beta} - \alpha_R [\mathbf{p} \times \boldsymbol{\sigma}_{\alpha\beta}]_z \right] \times \psi_{\beta, \mathbf{p}}^{(B)}(z) = 0; \quad (4)$$

and in the superconductor ($z \leq -a$),

$$\left(\varepsilon - \xi_{\mathbf{p}}^{(S)} + \frac{\hbar^2 \partial_z^2}{2m_S} \right) \psi_{\alpha, \mathbf{p}}^{(S)}(z) - \Delta_{\alpha\beta} \psi_{\beta, -\mathbf{p}}^{(S)\dagger}(z) = 0. \quad (5)$$

Here, $\mathbf{p} = (p_x, p_y)$ is the two-dimensional momentum parallel to the interface, $\hat{\boldsymbol{\sigma}} = (\hat{\sigma}_x, \hat{\sigma}_y, \hat{\sigma}_z)$ is the vector of Pauli matrices acting in spin space, $\xi_{\mathbf{p}}^{(F)} = \mathbf{p}^2/2m_F - \mu_F$ and $\xi_{\mathbf{p}}^{(S)} = \mathbf{p}^2/2m_S - \mu_S$ are the electronic spectra in the ferromagnet and superconductor, m_F , m_S and m_B are the effective masses in the corresponding region and μ_F and μ_S are the Fermi levels in the ferromagnet and superconductor. α and β here label the spin projections. We assume that the ferromagnet and superconductor are separated by a tunnel barrier of height U_0 that, due to mirror asymmetry with respect to reflections relative to the $z = -a/2$ plane, contains Rashba spin-orbit coupling characterized by parameter α_R . The ferromagnet is modeled as a Fermi gas in a Zeeman field \mathbf{h} . Finally, the superconductor is assumed to be of s -wave type and, consequently, the mean-field order parameter is momentum independent and reads $\Delta_{\alpha\beta} = \Delta(i\sigma_{y, \alpha\beta})$.

Although the barrier is spin-orbit coupled, this coupling will not lead to any spin Hall effects at the bound-

aries $z = 0$ and $z = -a$. Consequently, there is no accumulation of spin and the basic ballistic boundary conditions are identical to those in the theory of a conventional tunnel junction, namely:

$$\psi_{\alpha,\mathbf{p}}^{(F)}(d) = 0, \quad (6)$$

$$\psi_{\alpha,\mathbf{p}}^{(F)}(0) = \psi_{\alpha,\mathbf{p}}^{(B)}(0), \quad \psi_{\alpha,\mathbf{p}}^{(B)}(-a) = \psi_{\alpha,\mathbf{p}}^{(S)}(-a), \quad (7)$$

$$\frac{1}{m_F} \partial_z \psi_{\alpha,\mathbf{p}}^{(F)}(0) = \frac{1}{m_B} \partial_z \psi_{\alpha,\mathbf{p}}^{(B)}(0), \quad (8)$$

and

$$\frac{1}{m_B} \partial_z \psi_{\alpha,\mathbf{p}}^{(B)}(-a) = \frac{1}{m_S} \partial_z \psi_{\alpha,\mathbf{p}}^{(S)}(-a). \quad (9)$$

The full set of equations (3)-(5) is formulated for electron field operators acting in Fock space. However, since these equations and boundary conditions (6)-(9) are all linear, the operator nature of the unknown functions is not germane and we may simply approach the problem as in single-particle quantum mechanics. The problem is then conceptually very simple and reduces to solving second-order differential equations albeit with non-trivial boundary conditions. This can be done exactly to a large degree.

B. Deriving closed boundary conditions for the ferromagnet

1. Tunnel barrier

Let us look for a solution in the tunnel barrier in the following form, $\psi_{\alpha,\mathbf{p}}^{(B)}(z) = Z(z)\mathcal{P}_\alpha(\mathbf{p})$, where the transverse wave function $Z(z)$ satisfies

$$-\frac{\hbar^2}{2m_B} Z'' + [U_0 - \varepsilon + \varepsilon^R(\mathbf{p})]Z = 0, \quad (10)$$

and the planar wave function $\mathcal{P}_\alpha(\mathbf{p})$ is a standard wave function of the Rashba problem,

$$\mathcal{P}^\pm(\mathbf{p}) = \frac{1}{\sqrt{2}} \begin{pmatrix} \pm 1 \\ -ie^{i\gamma_{\mathbf{p}}} \end{pmatrix}, \quad (11)$$

describing the helicity eigenstates with eigenvalues, $\varepsilon_\pm^R(\mathbf{p}) = \frac{\mathbf{p}^2}{2m_B} \pm \alpha_R |\mathbf{p}|$. The angle $\gamma_{\mathbf{p}}$ is defined via $\mathbf{p} = p(\cos \gamma_{\mathbf{p}}, \sin \gamma_{\mathbf{p}})$. The general solution in the barrier then reads

$$\psi_{\alpha,\mathbf{p}}^{(B)}(z) = [C_{++}e^{q_+z} + C_{+-}e^{-q_+z}] \mathcal{P}_\alpha^+(\mathbf{p}) + [C_{-+}e^{q_-z} + C_{--}e^{-q_-z}] \mathcal{P}_\alpha^-(\mathbf{p}), \quad (12)$$

where $q_\pm = \sqrt{\frac{2m_B}{\hbar^2} [U_0 - \varepsilon + \varepsilon_\pm^R(\mathbf{p})]}$. To guarantee real q_\pm we assume that the spin-orbit interaction scale is smaller than the barrier height.

We now use (7) to determine the relations between the coefficients in (12) and the values of the wave function on the superconductor and ferromagnet boundaries. We find

$$C_{ll'} = \frac{l'}{4 \sinh(q_l a)} \left(\mathcal{F}^l e^{l' q_l a} - \mathcal{S}^l \right), \quad (13)$$

where $l, l' = \pm$ and

$$\mathcal{F}^\pm = i\psi_{\downarrow,\mathbf{p}}^{(F)}(0)e^{-i\gamma_{\mathbf{p}}} \pm \psi_{\uparrow,\mathbf{p}}^{(F)}(0); \quad (14)$$

$$\mathcal{S}^\pm = i\psi_{\downarrow,\mathbf{p}}^{(S)}(-a)e^{-i\gamma_{\mathbf{p}}} \pm \psi_{\uparrow,\mathbf{p}}^{(S)}(-a). \quad (15)$$

2. Superconductor

We now match the tunnel-barrier solution (12) with the superconducting solution at the barrier-superconductor interface using boundary condition (9). We then find

$$\frac{m_B}{m_S} \psi_{\alpha,\mathbf{p}}^{(S)}(-a) = T_{\mathbf{p},\alpha\beta} \psi_{\beta,\mathbf{p}}^{(F)}(0) - R_{\mathbf{p},\alpha\beta} \psi_{\beta,\mathbf{p}}^{(S)}(-a). \quad (16)$$

The matrices in (16), which play an important role in the analysis of the Andreev scattering problem, are given by

$$\hat{T}_{\mathbf{p}} = \begin{pmatrix} \kappa_t & i\delta\kappa_t e^{-i\gamma_{\mathbf{p}}} \\ -i\delta\kappa_t e^{i\gamma_{\mathbf{p}}} & \kappa_t \end{pmatrix} \quad (17)$$

$$\hat{R}_{\mathbf{p}} = \begin{pmatrix} \kappa & i\delta\kappa e^{-i\gamma_{\mathbf{p}}} \\ -i\delta\kappa e^{i\gamma_{\mathbf{p}}} & \kappa \end{pmatrix}. \quad (18)$$

Here, we have defined

$$\kappa_t = \frac{q_+}{2 \sinh(q_+ a)} + \frac{q_-}{2 \sinh(q_- a)} \quad (19)$$

$$\delta\kappa_t = \frac{q_+}{2 \sinh(q_+ a)} - \frac{q_-}{2 \sinh(q_- a)} \quad (20)$$

and

$$\kappa = \frac{q_+}{2 \tanh(q_+ a)} + \frac{q_-}{2 \tanh(q_- a)} \quad (21)$$

$$\delta\kappa = \frac{q_+}{2 \tanh(q_+ a)} - \frac{q_-}{2 \tanh(q_- a)}, \quad (22)$$

with q_\pm^{-1} being the penetration length of a particle with a positive/negative chirality inside the barrier, and a is the barrier width. As the width of the barrier grows, the “tunneling” boundary coefficients decay exponentially, $\lim_{a \rightarrow \infty} \kappa_t = 0$. As expected, we see then that the coupling between the superconductor and the ferromagnet disappears, as does the proximity effect. Furthermore, if we “turn off” the spin-orbit coupling in the barrier (i.e. setting $\alpha_R = 0$, so that $q_+ = q_-$), we see that the spin-mixing terms vanish, $\delta\kappa = \delta\kappa_t = 0$, and we recover the standard boundary conditions for the proximity effect.

To describe the superconductor [see (5)] we introduce a four-component state-vector in the combined spin-Nambu space,

$$\vec{\Psi}_{\mathbf{p}}(z) = \left(\psi_{\uparrow,\mathbf{p}}^{(S)}(z), \psi_{\downarrow,\mathbf{p}}^{(S)}(z), \psi_{\uparrow,-\mathbf{p}}^{(S)*}(z), \psi_{\downarrow,-\mathbf{p}}^{(S)*}(z) \right)^T.$$

The Pauli matrices in Nambu space will be denoted by $\hat{\tau}_x$, $\hat{\tau}_y$ and $\hat{\tau}_z$, and the unit matrix by $\hat{\tau}_0$. 4×4 matrices in the spin-Nambu space will be denoted by an inverse hat, for instance,

$$\check{T}_{\mathbf{p}} = \begin{pmatrix} \hat{T}_{\mathbf{p}} & 0 \\ 0 & \hat{T}_{-\mathbf{p}}^* \end{pmatrix}, \quad \check{R}_{\mathbf{p}} = \begin{pmatrix} \hat{R}_{\mathbf{p}} & 0 \\ 0 & \hat{R}_{-\mathbf{p}}^* \end{pmatrix}, \quad (23)$$

where the asterisk denotes complex conjugation. Note that $\gamma_{-\mathbf{p}} = \gamma_{\mathbf{p}} + \pi$, therefore, $\exp(i\gamma_{-\mathbf{p}}) = -\exp(i\gamma_{\mathbf{p}})$, as it appears in $\hat{T}_{-\mathbf{p}}^*$ and $\hat{R}_{-\mathbf{p}}^*$.

Using these notations, we can write the boundary conditions for the superconductor in the following compact form, $\frac{m_B}{m_S} \partial_z \vec{\Psi}_{\mathbf{p}}^{(S)}(-a) = \check{T}_{\mathbf{p}} \vec{\Psi}_{\mathbf{p}}^{(F)}(0) - \check{R}_{\mathbf{p}} \vec{\Psi}_{\mathbf{p}}^{(S)}(-a)$. We proceed by first incorporating the right side of this boundary condition into the Bogoliubov-de Gennes equation for a superconductor, which we symbolically write in the form,⁵⁰

$$\check{G}_{\mathbf{p}}^{-1} \vec{\Psi}_{\mathbf{p}}^{(S)}(z) = -\frac{\hbar^2}{2m_B} \delta(z+a) \left[\check{T}_{\mathbf{p}} \vec{\Psi}_{\mathbf{p}}^{(F)}(0) - \check{R}_{\mathbf{p}} \vec{\Psi}_{\mathbf{p}}^{(S)}(-a) \right]. \quad (24)$$

Here, $\check{G}_{\mathbf{p}}(z, z')$ is the Green function of the Bogoliubov-de Gennes equation for a bulk superconductor in the half-space, $z < -a$, which satisfies the von Neumann boundary conditions, $\partial_z \check{G}_{\mathbf{p}}(z, z') \Big|_{z=-a} = 0$. It can be expressed in terms of the Green function of an infinite bulk s -wave superconductor by the method of mirror images and reads,

$$\check{G}_{\mathbf{p}}(z, z') = \check{G}_{\mathbf{p}}(z - z') + \check{G}_{\mathbf{p}}(z + z' + 2a), \quad (25)$$

where

$$\check{G}_{\mathbf{p}} = \begin{pmatrix} \hat{G}_{\mathbf{p}} & \hat{F}_{-\mathbf{p}}^* \\ \hat{F}_{\mathbf{p}} & \hat{G}_{-\mathbf{p}}^* \end{pmatrix} \quad (26)$$

and $\hat{G}_{\mathbf{p}}$ and $\hat{F}_{\mathbf{p}}$ are the normal and Gor'kov Green functions, respectively. Consequently, the solution to the Bogoliubov-de Gennes equation (24) is derived by convoluting the Green function with the boundary term on the right side of (24), which is simple due to the delta-function in the latter,

$$\vec{\Psi}_{\mathbf{p}}^{(S)}(z) = -\frac{\hbar^2}{m_B} \check{G}_{\mathbf{p}}(z+a) \left[\check{T}_{\mathbf{p}} \vec{\Psi}_{\mathbf{p}}^{(F)}(0) - \check{R}_{\mathbf{p}} \vec{\Psi}_{\mathbf{p}}^{(S)}(-a) \right]. \quad (27)$$

For the purpose of understanding induced superconductivity in the ferromagnet we only need to know the boundary value of the superconducting wave function at $z = -a$. From (27) we obtain

$$\vec{\Psi}_{\mathbf{p}}^{(S)}(-a) = -\frac{\hbar^2}{m_B} \frac{1}{1 - (\hbar^2/m_B) \check{g}_{\mathbf{p}} \check{R}_{\mathbf{p}}} \check{g}_{\mathbf{p}} \check{T}_{\mathbf{p}} \vec{\Psi}_{\mathbf{p}}^{(F)}(0), \quad (28)$$

where

$$\check{g}_{\mathbf{p}} = \lim_{z \rightarrow -a} \check{G}_{\mathbf{p}}(z+a) = \int \frac{dp_z}{2\pi} \check{G}(p_x, p_y, p_z). \quad (29)$$

We note here that (28) is *exact* and that we have not used any properties of the system at $z > 0$ up to this point. Therefore, the equation above is applicable to any such junction with any normal or superconducting material at $z > 0$ (the only constraint is the continuity of derivatives at the $z = 0$ boundary, which may be violated if there is a spin Hall effect present. In this case, however, an alternative set of boundary conditions can be derived).

3. Ferromagnet

The expression in (28), which represents a useful technical result of the paper, allows one to formulate a closed problem on the (ferromagnetic) normal side. Let us write the Schrödinger equation (3) as

$$\check{G}_{\mathbf{p}}^{(F)-1} \circ \vec{\Psi}_{\mathbf{p}}^{(F)}(z) = 0, \quad (30)$$

where we have extended the equation into the Nambu space. The propagator $\check{G}_{\mathbf{p}}^{(F)}(z, z')$ describes a particle of the magnetized Fermi liquid in the shell $0 \leq z \leq d$. Apart from the trivial boundary condition (6) at the hard wall, (8) together with the solution of Sec. IIIB 1 and (28) give rise to the following constraint,

$$\frac{m_B}{m_F} \partial_z \vec{\Psi}_{\mathbf{p}}^{(F)}(0) = \left[\check{R}_{\mathbf{p}} + \check{T}_{\mathbf{p}} \frac{\hbar^2/m_B}{1 - \frac{\hbar^2}{m_B} \check{g}_{\mathbf{p}} \check{R}_{\mathbf{p}}} \check{g}_{\mathbf{p}} \check{T}_{\mathbf{p}} \right] \vec{\Psi}_{\mathbf{p}}^{(F)}(0). \quad (31)$$

The boundary condition (9) together with (30) and (31) form a self-consistent set for $z > 0$.

We assume at this point that the spin-orbit coupling energy scale is small compared to other relevant energies in the problem and keep the spin-orbit parameter α_R finite only where we otherwise would get a vanishing effect, i.e. in the spin-mixing terms. In all other quantities, we set $\alpha_R = 0$. This brings the reflection matrix to a simpler form proportional to the unit matrix,

$$\check{R}_{\mathbf{p}} \approx \kappa \check{1} \equiv \kappa \hat{\tau}_0 \hat{\sigma}_0, \quad (32)$$

where κ is defined in (21). In the $\alpha_R \rightarrow 0$ limit we have $\kappa = q / \tanh(qa)$, where $q = \sqrt{\frac{2m}{\hbar^2} (U_0 + \frac{\mathbf{p}^2}{2m_B} - \varepsilon)}$. In the limit of a high barrier, $\kappa \approx q$.

We now consider the operator denominator in the boundary condition (31). If the bulk superconductor is deep in the paired state, we may neglect the normal Green function and estimate the integrated Green function in (29) as $\check{g} \approx f \hat{\tau}_x (i \hat{\sigma}_y)$, with

$$f = \frac{1}{2\hbar v_S} \frac{\Delta}{\sqrt{\Delta^2 + \xi_{\mathbf{p}}^2}}. \quad (33)$$

For small $\xi_{\mathbf{p}} = p^2/(2m_S) - \mu_S$, it can be estimated as $f \approx 1/(2\hbar v_S)$, where v_S is the Fermi velocity in the superconductor. Therefore, the term in question from (31) becomes

$$\frac{\hbar^2}{m_B} \frac{1}{1 - \frac{\hbar^2}{m_B} \check{\mathbf{p}} \check{\mathbf{R}}_{\mathbf{p}}} \check{\mathbf{g}}_{\mathbf{p}} \approx \frac{1}{\kappa} \frac{\alpha}{1 + \alpha^2} [\hat{\tau}_x (i\hat{\sigma}_y) - \alpha \hat{1}], \quad (34)$$

where $\alpha = \kappa f/m_B$. This parameter can be estimated as $\alpha \sim \sqrt{m_S U_0/m_B E_F^{(S)}}$. Note that the last term in (34) is uninteresting because it does not include any off-diagonal contributions in Nambu space. The term slightly renormalizes the boundary conditions for the transverse wave function in the ferromagnet. It can therefore be safely dropped.

Incorporating the right side of the boundary condition (31) into the Schrödinger equation for the ferromagnet (30) we obtain

$$\check{G}_{\mathbf{p}}^{(F)-1} \circ \vec{\Psi}_{\mathbf{p}}^{(F)}(z) = \frac{-\hbar^2 \alpha \delta(z)}{2f\kappa m_B(1 + \alpha^2)} \check{T}_{\mathbf{p}} \check{\mathbf{g}}_{\mathbf{p}} \check{T}_{\mathbf{p}} \vec{\Psi}_{\mathbf{p}}^{(F)}(0). \quad (35)$$

This is the Bogoliubov-de Gennes equation for the normal region with superconducting correlations introduced via the boundary term that carries information about all Andreev processes.

C. Proximity-induced superconducting gap

In order to calculate the superconducting gap induced in the ferromagnet, we assume that its magnetization is unaffected by the proximity to the superconductor and fix it instead of calculating it self-consistently. We also focus on a particular sub-band with a given spin polarization and ignore intraband scattering (which is justified only in the clean case). Furthermore, we assume that the ferromagnetic layer or wire is very thin in the z -direction and approximate the full solution as

$$\psi_{\alpha, \mathbf{p}}^{(F)}(z) = \chi_{\alpha}(\mathbf{m}) \psi^{(\text{tr})}(z) \phi(\mathbf{p}), \quad (36)$$

where $\chi_{\alpha}(\mathbf{m})$ is a spinor describing the magnetization direction that we wish to enforce and $\psi^{(\text{tr})}(z)$ is the transverse envelope wave function that we approximate as a solution of the free one-dimensional Schrödinger equation,

$$\left(\partial_z^2 + \frac{2m_F \varepsilon_{\text{tr}}}{\hbar^2} \right) \psi^{(\text{tr})}(z) = 0, \quad (37)$$

with the unusual boundary conditions,

$$\frac{m_B}{m_F} \partial_z \psi^{(\text{tr})}(0) = \kappa \psi^{(\text{tr})}(0), \quad \psi^{(\text{tr})}(d) = 0. \quad (38)$$

We then introduce solution (36) into (35), multiply it by $\psi^{(\text{tr})*}(z)$, average it over the transverse direction, and extract the relevant spin component (a word caution here is that the standard convention for the Gor'kov Green

function taken proportional to $i\hat{\sigma}_y$ is basis-dependent and assumes spin quantization along the z -axis).

For the ferromagnetic state polarized along z , we obtain the Bogoliubov-de Gennes equations in the familiar form,

$$\left[\frac{\mathbf{p}^2}{2m_F} - (\mu_F - \varepsilon_{\text{tr}}) \right] \phi_{\mathbf{p}} + E_g (p_y + ip_x) \phi_{-\mathbf{p}}^* = 0, \quad (39)$$

where the proximity-induced gap or so-called minigap is

$$E_g = \frac{f\hbar^4}{pm_B^2} \kappa_t \delta \kappa_t \left| \psi^{(\text{tr})}(0) \right|^2. \quad (40)$$

The boundary value of the transverse wave function can be obtained from (37) and reads

$$\left| \psi^{(\text{tr})}(0) \right|^2 = \frac{2}{d} \frac{1}{1 + \xi^2 + \xi/(k_{\text{tr}}d)}, \quad (41)$$

where $\xi = m_F q/(m_B k_{\text{tr}})$ and k_{tr} is a solution to the eigenvalue problem, $\tan(k_{\text{tr}}d)/(k_{\text{tr}}d) = -m_B/(m_F qd)$, which determines the spectrum, $\varepsilon_{\text{tr}} = \hbar^2 k_{\text{tr}}^2/(2m_B)$. We see from Eq. (40) that the proximity-induced minigap is extremely sensitive to the actual width of the normal region: the smaller the width, the more frequent Andreev scattering processes, and the larger the minigap.⁵⁰

IV. RESISTANCE PEAK DUE TO SUPERCONDUCTING FLUCTUATIONS

We argued in Sec. II B that the W electrodes have a strong impact on the transport properties through the Co wire. We reiterate the experimental fact that when an extra W strip is deposited on top of the Co wire [see Fig. 1(c)], the normal state resistance of the wire increases by nearly 50%. This indicates that when a W electrode is deposited onto a nanowire they modify the wire in its vicinity and provide a major source of resistance. A faithful model of the Co wire may then be such that the current i_w goes through the two W voltage electrodes. If this view is adopted this creates four W-Co interfaces, each one similar to the interface considered in Sec. III. With this geometry electron transport through the wire is expected to be strongly modified by Andreev physics at the W-Co interfaces.

We now focus on the resistance peak observed near the superconducting transition temperature of the W electrodes. This peak is very reminiscent of similar anomalous peaks studied in the context of c -axis transport in cuprate superconductors^{51–53}, magnetoresistance in dirty films⁵⁴, as well as magnetoresistance in granular electronic systems⁵⁵. In all these cases, the anomalous peak has been explained using the phenomenon of superconducting fluctuations.^{41,42} This phenomenon is concerned with fluctuating Cooper pairs that form while the system is in the normal state, either just above the transition temperature T_c or the critical magnetic field H_c . For the

$H = 0$ case, the appearance of Cooper pairs above T_c opens up a new channel for charge transport. Indeed, these fluctuating Cooper pairs can be treated as carriers of charge $2e$ with a lifetime given by $\tau_{\text{GL}} \sim \hbar/k_B(T - T_c)$. This leads to a contribution to the conductivity known as the Aslamazov-Larkin (AL) contribution or paraconductivity, and gives a positive correction to the Drude conductivity. There is also an indirect correction known as the density of states (DOS) contribution. One of the important consequences of these fluctuating Cooper pairs is the decrease in single-particle DOS near the Fermi level. The idea is that if some electrons are involved in pairing they can not simultaneously participate in single-electron transport. The DOS contribution therefore gives a negative correction to the Drude conductivity.

As we approach T_c of the W electrodes, Cooper pair fluctuations grow inside the W electrodes. By virtue of the Rashba spin-orbit coupling at the W-Co interfaces (due to breaking of mirror symmetry in the longitudinal direction at the interface) singlet Cooper pairs inside W are converted and triplet fluctuations permeate into the Co wire. AL correction to the conductivity arises due to the transport of these fluctuating Cooper pairs through the wire. However, Cooper pair tunneling across an interface is strongly suppressed because it is a higher-order process in both tunneling and the singlet-triplet conversion rate, which requires a spin flip process enabled only by weak interfacial spin-orbit coupling. This can be seen in (17) where the off-diagonal elements of the transmission matrix are suppressed by the factor $\delta\kappa_t$, which is proportional to α_R . The single electron tunneling and the DOS correction, on the other hand, are lower order tunneling processes that require no spin flipping. We therefore qualitatively expect the DOS correction to be parametrically larger than the AL contribution, thus giving a negative overall correction to the Drude conductivity. This clearly can explain the anomalous upturn in the resistance as a function of temperature.

When the Co wire is replaced by a gold wire, the situation is modified. Since gold is not ferromagnetic, s -wave pairing correlations are expected to survive over a much longer distance inside the wire. In this case, Cooper pair tunneling through the W-Au interface is much more transparent since it does not require spin flipping. Therefore, Cooper pairs are more efficient at transporting charge in this case, and the AL contribution to the conductivity is expected to play a much bigger role than with a ferromagnetic wire. Here, we purport that the absence of the resistance peak in the Au wire can be explained if indeed the AL contribution to the conductivity is parametrically larger than the DOS contribution, thus giving an overall positive correction to the conductivity.

Near the superconducting transition temperature (and at $H = 0$) and in dimensions at or below two, both AL and DOS contributions show either algebraic or logarithmic divergent behavior as a function of the distance from the transition point. Denoting the divergent part of the

AL corrections by function $f_{\text{AL}}(T - T_c)$ and the divergent part of the DOS correction by $f_{\text{DOS}}(T - T_c)$ (and ignoring the Maki-Thompson contribution), the total superconducting fluctuation correction to the normal resistance R_0 can be schematically written as

$$\frac{\delta R(T)}{R_0} = A_{\text{DOS}} f_{\text{DOS}}(T - T_c) - A_{\text{AL}} f_{\text{AL}}(T - T_c), \quad (42)$$

where, A_{AL} and A_{DOS} are positive pre-factors. As we will show in Sec. IV A,

$$f_{\text{AL}} \sim \frac{1}{(T/T_c - 1)^4}, \quad (43)$$

while

$$f_{\text{DOS}} \sim \frac{1}{\sqrt{T/T_c - 1}}, \quad (44)$$

indicating that the AL contribution diverges much more strongly than the DOS term as $T \rightarrow T_c^+$. Therefore, unless the pre-factor A_{AL} is exceedingly small in comparison to A_{DOS} the DOS contribution is always parametrically smaller than the AL contribution and the conductivity correction is positive. This leads to a monotonic decrease in the resistance as the system approaches the transition, and no peak will result. However, if we have a situation where the AL pre-factor is greatly suppressed, i.e. $A_{\text{AL}} \ll A_{\text{DOS}}$, the DOS contributions may become parametrically larger than the AL counterpart for T sufficiently, but not too close to T_c^+ . In this case, the resistivity can display an anomalous upturn before the AL contribution eventually takes over and the resistivity makes a precipitous fall as $T \rightarrow T_c^+$.

A. Microscopic theory

1. Effective dimensionality of a tungsten electrode for fluctuation analysis

The superconducting fluctuation physics depends critically on the dimensionality of the system, with the general trend being that the lower the dimensionality, the more pronounced and singular the fluctuation effects are. However, one should exercise care in determining the effective dimensionality of a system, as this notion depends on a particular effect that is being studied. For example, the system may be three-dimensional in terms of single-electron diffusion physics, but fall into the category of one-dimensional superconductors when it comes to the fluctuation analysis. We believe that such is the case with the W electrodes that host superconductivity and most of the fluctuation physics in the experiment under study involving $L_{\perp}^{(1)} \sim 250\text{nm}$ wide and $L_{\perp}^{(2)} \sim 100\text{nm}$ thick W strips.

The finiteness of the transverse directions implies that whenever we have an integral over a three-dimensional

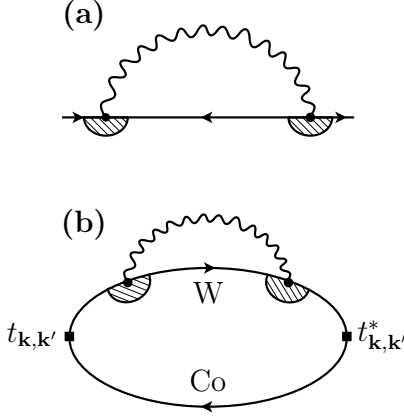


FIG. 4: (a) Self-energy diagram describing a correction to the single-electron Green function. The wavy line corresponds to the superconducting fluctuation propagator, and the shaded vertices represent Cooperon vertices. (b) A diagram corresponding to the lowest-order correction to the transport kernel due to superconducting fluctuations in the tungsten electrode. As labeled in the figure, top (bottom) solidline represents the electron propagator for tungsten (cobalt).

momentum, its transverse part must be replaced with a sum over quantized modes,

$$\int \frac{dq_{\perp}}{2\pi\hbar} f(q_{\perp}) \longrightarrow \frac{1}{L_{\perp}} \sum_{n_{\perp}} f\left(\frac{2\pi\hbar n_{\perp}}{L_{\perp}}\right).$$

For superconducting fluctuation analysis, the relevant function of interest is the fluctuation propagator, which appears in the combination

$$\frac{1}{L_{\perp}} \sum_{n_{\perp}} \left[D \left(\frac{2\pi\hbar n_{\perp}}{L_{\perp}} \right)^2 + Dq_{\parallel}^2 + \tau_{\text{GL}}^{-1} \right]^{-1}, \quad (45)$$

where $D = v_F^2\tau/3$ is the diffusion coefficient and the Ginzburg-Landau relaxation time,

$$\tau_{\text{GL}} = \frac{\pi}{8} \frac{\hbar}{T - T_c}, \quad (46)$$

tunes the proximity to the transition temperature T_c . Hereafter, we will focus on a superconducting electrode and assume that we are dealing there with a disordered superconductor.

The question of whether or not a particular dimension is important reduces to the comparison of the first and last term in the square brackets in (45). If the former is much larger than the latter for any $n_{\perp} \neq 0$ the corresponding dimension is unimportant and an effective reduction of dimensionality occurs. One can define the following characteristic temperature scale (to be compared with $T - T_c$)

as follows

$$T_{\perp}(L_{\perp}) = \frac{1}{k_B} \left(\frac{\pi^3}{6} \right) \left(\frac{l}{L_{\perp}} \right) \left(\frac{\hbar v_F}{L_{\perp}} \right), \quad (47)$$

where v_F is the Fermi velocity, $l = v_F\tau$ is the electron mean-free path and we have restored the Boltzmann constant k_B and the Planck constant \hbar .

For W, the Fermi velocity can be estimated as $v_F \sim 0.5 \cdot 10^6$ m/s and taking the largest of the two transverse dimensions $L_{\perp} \sim 250$ nm, we find

$$T_{\perp}^W(250\text{nm}) \sim \left(\frac{l}{L_{\perp}} \right) 80 \text{ K}.$$

If we assume that the mean-free path in the amorphous W strips is of order a nanometer the corresponding temperatures scale becomes of order $T_{\perp}^W(250\text{nm}) \sim 0.3\text{-}1\text{K}$, which is very reasonable and implies that as soon as we approach the superconducting transition with $(T - T_c) \ll T_c \sim 4.4\text{-}5\text{K}$, we may view the electrode as a one-dimensional superconductor.

2. Fluctuation correction to the density of states

We now analyze the DOS fluctuation physics on the basis of the standard diagrammatic perturbation theory. The Cooper-channel correction to the electronic DOS is given by

$$\delta\nu(\epsilon) = -\frac{1}{\pi} \int \frac{d^d p}{(2\pi)^d} \text{Im} \{ \mathcal{G}^2(i\epsilon_m, \mathbf{p}) \Sigma(i\epsilon_m, \mathbf{p}) \} \Big|_{i\epsilon_m \rightarrow \epsilon}, \quad (48)$$

where $\Sigma(i\epsilon_m, \mathbf{p})$ is the self-energy described by the diagram in Fig. 4(a). It reads

$$\Sigma(i\epsilon_m, \mathbf{p}) = -T \sum_{\Omega_n} \int \frac{d^d q}{(2\pi)^d} \mathcal{G}(i\Omega_n - i\epsilon_m, \mathbf{q} - \mathbf{p}) \times \mathcal{C}(\epsilon_m, \Omega_n - \epsilon_m; \mathbf{q}) \mathcal{L}(\Omega_n, \mathbf{q}), \quad (49)$$

where

$$\mathcal{G}(i\epsilon_m, \mathbf{p}) = \frac{1}{i\tilde{\epsilon}_m - \xi_{\mathbf{p}}} \quad (50)$$

is the Matsubara Green function with $\xi_{\mathbf{p}} = v_F(p - p_F)$ and $\tilde{\epsilon}_m = \epsilon_m + \text{sgn}(\epsilon_m)/(2\tau)$ and τ is the scattering time,

$$\mathcal{C}(\epsilon_m, \Omega_n - \epsilon_m; \mathbf{q}) = \frac{1}{\tau} \frac{\theta[\epsilon_m(\epsilon_m - \Omega_n)]}{Dq^2 + \gamma_s + |\epsilon_m - \Omega_n|} \quad (51)$$

is the Cooperon vertex, where we included pair-breaking scattering rate $\gamma_s = 2/\tau_s$ and $\theta(\cdot)$ is the standard Heaviside step function. In the vicinity of the transition point the fluctuation propagator reads

$$\mathcal{L}(\Omega_n, \mathbf{q}) = \frac{8T_c}{\pi\nu_0} [Dq^2 + \tau_{\text{GL}}^{-1} + |\Omega_n|]^{-1}, \quad (52)$$

where $\tau_{\text{GL}} = \frac{\pi}{8} \frac{\hbar}{T - T_c}$ and $\nu_0 = mp_F/2\pi^2$ is the bare DOS for a single spin projection. As per the usual convention, $\Omega_n = 2\pi nT$ denotes the bosonic Matsubara frequency and $\varepsilon_m = (2m + 1)\pi T$ is the fermionic Matsubara frequency. Finally, note that the physical quantity of interest, the DOS, must be analytically continued from the discrete set of Matsubara frequencies to the continuum of real energies, as labelled by the symbol $i\varepsilon_m \rightarrow \epsilon$ in (48).

Since the Tungsten electrodes are amorphous, we can safely assume that they are strongly disordered s -wave superconductors, where $T_c\tau \ll 1$ (but of course we also assume that we are far from localization, that is $E_F\tau \gg 1$). In this case, the three-Green-function block takes the especially simple form

$$\begin{aligned} \nu_0 \int d\xi \mathcal{G}(i\Omega_n - i\varepsilon_m, \mathbf{q} - \mathbf{p}) \mathcal{G}^2(i\varepsilon_m, \mathbf{p}) \\ = -2\pi i \nu_0 \tau^2 \text{sgn}(\varepsilon_m), \end{aligned} \quad (53)$$

where we enforced the constraint $\varepsilon_m(\varepsilon_m - \Omega_n) > 0$ in (51). This leads to the following expression for the DOS

$$\delta\nu(\epsilon) = \frac{4}{\pi^3} \int \frac{d^d q}{(2\pi)^d} \left(\frac{\partial}{\partial \gamma_s} \right) \text{Re } S^R(\mathbf{q}, \epsilon), \quad (54)$$

where $S^R(\mathbf{q}, \epsilon) = S(\mathbf{q}, i\varepsilon_m \rightarrow \epsilon)$ represents the analytically-continued (retarded) Matsubara sum

$$\begin{aligned} S(\mathbf{q}, \varepsilon_m > 0) \\ = \sum_{n=-\infty}^m \frac{1}{\left(\frac{Dq^2 + \tau_{\text{GL}}^{-1}}{2\pi T_c} + |n| \right) \left(\frac{Dq^2 + \gamma_s}{2\pi T_c} + |2m + 1 - n| \right)}. \end{aligned} \quad (55)$$

This sum can be calculated exactly in terms of the digamma function,

$$\psi(z) = -\gamma + \sum_{n=0}^{\infty} \left[(n+1)^{-1} - (n+z)^{-1} \right], \quad (56)$$

which is analytic everywhere except $z = 0, -1, -2, \dots$. It is convenient to separate the sum (55) into two pieces, $\sum_{n=-\infty}^0 \dots$ and $\sum_{n=0}^m \dots$. For the first term analytic continuation reduces to replacing $\varepsilon_m \rightarrow -i\varepsilon$. For the second term it becomes possible after noticing the “reflection property”, where $m - n$ can be replaced by $n - m$. This leaves the sum from $n = 0$ to $n = m$ unchanged but the denominator “positively-defined” and ready for analytic continuation. Finally, the asymptotic form of DOS in the limit of $\{\epsilon, \tau_{\text{GL}}^{-1}, \gamma_s\} \ll T \sim T_c$ becomes

$$S^R(\mathbf{q}, \epsilon) = \frac{(2\pi T_c)^2}{(Dq^2 + \tau_{\text{GL}}^{-1})(2Dq^2 + \gamma_s + \tau_{\text{GL}}^{-1} - 2i\epsilon)}. \quad (57)$$

Let us now focus specifically on the correction to the DOS of electronic states with spin-up at the Fermi level, i.e. $\epsilon = 0$. The remaining elementary integrals in (54) can now be easily calculated and we find

$$\delta\nu_{\uparrow}(0, T) = -\frac{\nu_0}{p_F^2 A} \frac{\sqrt{6\pi^7}}{128} \frac{T_c^2 \tau^{-1/2}}{(T - T_c)^{5/2}} \frac{1 + 2\alpha(T)}{\alpha^3(T) [1 + \alpha(T)]^2}, \quad (58)$$

where

$$\alpha(T) = \sqrt{\frac{1}{2} \left[1 + \frac{\pi}{4} \frac{1}{(T - T_c) \tau_s} \right]}. \quad (59)$$

Here, A is the effective area of the fluctuating superconductor in the region where the fluctuations are studied (we expect it to be related to the dimensions of the superconductor-nanowire contact and, consequently, expect A to be smaller than the cross-sectional area of the wire). Notice that in the absence of pair breaking and/or far from the transition, where $(T - T_c) \tau_s \gg 1$, (59) reduces to a constant $\alpha = 1/\sqrt{2}$ and the DOS at the Fermi level acquires a very sharp temperature dependence as follows:

$$\delta\nu_{\uparrow}(0, T) \propto -(T - T_c)^{-5/2}, \text{ if } (T - T_c) \tau_s \gg 1. \quad (60)$$

In the opposite regime of strong pair-breaking scattering or in the immediate vicinity of the transition, we find

$$\delta\nu_{\uparrow}(0, T) \propto -(T - T_c)^{-1/2}, \text{ if } (T - T_c) \tau_s \ll 1. \quad (61)$$

3. Fluctuation correction to the contact resistance

The result for the DOS at the Fermi level provides a useful insight into the physics near the transition and illustrates that, as a precursor to the global pairing transition, electrons are actively swept from the vicinity of the Fermi level due to the formation of the fluctuating Cooper pairs. However, the stand-alone quantity $\delta\nu(0, T)$ is not extremely useful for comparison with experiment, as it is actually not directly measurable. What is measured in experiment is resistance, which is an integral quantity that includes excitations with different energies and that has contributions from both single-electron transport across the W-Co junction and pair transport. As found in Sec. III, the latter is suppressed strongly far from the transition due to the very small pair tunneling probability, which requires spin-orbit-assisted spin flips. Single-electron transport on the other hand does not rely on any spin-orbit coupling, and spin-up electrons can tunnel freely from the electrodes into the ferromagnet. Hence, there is a regime close to the transition (but still far enough from the immediate vicinity, where the Cooper pairs eventually take over) where the single-electron tunneling dominates and is already strongly suppressed by fluctuations. This results in the upturn in the resistance as $T \rightarrow T_c^+$.

If we now focus entirely on single-electron transport and disregard the pair-breaking scattering, one would tend to conclude (incorrectly) that the tunneling resistance acquires a contribution proportional to that in (60). This, however, is not so and the correction to the conductance is much weaker. This is because the tunneling electrons involve not only those precisely at the Fermi level, but all electron excitations within the shell of energies $E \sim (E_F - T, E_F + T)$. Hence, what matters is

a redistribution of the DOS beyond the shell of energies that participate in transport (any redistribution within the shell is essentially not observable).

All these phenomena are automatically accounted for within the standard diagrammatic theory of transport. Here, we proceed nearly in a one-to-one correspondence with Ref. 56. The tunneling current is derived from the transport kernel $Q(\omega_l)$ shown in Fig. 4(b),

$$I(V) = -e \text{Im} Q^R(\omega) \Big|_{\omega=eV}, \quad (62)$$

where $Q^R(\omega)$ is analytically-continued transport kernel and V is the voltage across the tunneling contact. In the setup under consideration the Matsubara transport kernel reads explicitly

$$\begin{aligned} Q(\omega_l) &= -T^2 \sum_{\varepsilon_m; \Omega_n; \mathbf{k}, \mathbf{k}'} |t_{\mathbf{k}, \mathbf{k}'}|^2 \mathcal{G}_W^2(\varepsilon_m, \mathbf{k}) \mathcal{G}_{Co}(\varepsilon_m + \omega_l, \mathbf{k}') \\ &\times \int \frac{dq}{2\pi A} \mathcal{L}(\Omega_n, \mathbf{q}) \mathcal{C}^2(\varepsilon_m, \Omega_n - \varepsilon_m; \mathbf{q}) \\ &\times \mathcal{G}_W(\Omega_n - \varepsilon_m, \mathbf{q} - \mathbf{k}), \end{aligned} \quad (63)$$

where $t_{\mathbf{k}, \mathbf{k}'}$ is the tunneling amplitude between two momentum states, $\mathcal{G}_{W/Co}(\varepsilon_m, \mathbf{k})$ is the electron Green function for the W electrode/Co nanowire and all other quantities have been defined in Sec. IV A 2. Following Ref. 56 we introduce a normal state resistance of the W-Co junction $R_{W/Co}^{(0)}$ and obtain

$$\begin{aligned} Q(\omega_l) &= \frac{\pi T^2}{2e^2 R_{W/Co}^{(0)}} \sum_{\varepsilon_m, \Omega_n} \text{sgn}(\varepsilon_m) \text{sgn}(\varepsilon_m + \omega_l) \\ &\times \theta[\varepsilon_m(\varepsilon_m - \Omega_n)] \int \frac{dq}{2\pi A} \frac{\mathcal{L}(\Omega_n, \mathbf{q})}{(Dq^2 + |\varepsilon_m - \Omega_n|)^2}. \end{aligned} \quad (64)$$

Repeating the dimensionality-independent summations as in Ref. 56 (note that the clean case⁵⁶ becomes technically equivalent to the dirty case if we notice that the frequency-dependence of the three-Green-function block in the reference is identical to that in the two Cooperons that appear in (64)) and evaluating the remaining integral over momentum q we obtain the non-linear I - V dependence

$$\begin{aligned} I(V) &= -\frac{T}{8\pi^2 e} \sqrt{\frac{3\pi}{2}} \frac{1}{R_{W/Co}^{(0)} \nu_0 v_F A} \text{Im} \psi' \left[\frac{1}{2} - \frac{ieV}{2\pi T} \right] \\ &\times \frac{1}{\sqrt{(T - T_c)\tau}}, \end{aligned} \quad (65)$$

where $\psi(\cdot)$ is the logarithmic derivative of the gamma-function. Now focusing on the linear response regime, $\frac{dI}{dV}|_{V=0}$, we find the leading fluctuation correction to the W-Co contact resistance as follows,

$$\frac{\delta R_{W/Co}^{(DOS)}}{R_{W/Co}^{(0)}} = \frac{7\zeta(3)}{4\pi} \sqrt{\frac{3\pi}{2}} \frac{1}{p_F^2 A} \frac{1}{\sqrt{(T - T_c)\tau}}, \quad (66)$$

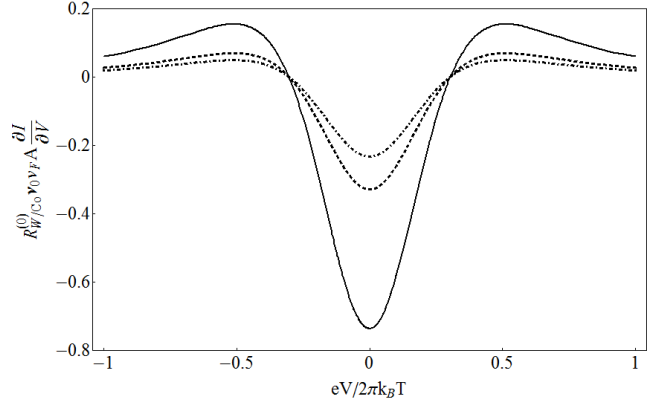


FIG. 5: Correction to the differential conductance from superconducting fluctuations as a function of dimensionless voltage $eV/2\pi T$ (see (65)). The three curves correspond to different temperatures: $t := (T - T_c)\tau = 0.01$ for the solid line; $t = 0.05$ for the dashed line; and $t = 0.1$ for the dotted line.

where $\zeta(z)$ is the Riemann zeta-function and $\zeta(3) \approx 1.202$. The result in (66) corresponds to a sharp upturn in the resistance upon approaching the superconducting transition of the electrode.

4. Estimate of tunneling resistance due to fluctuating pairs

As emphasized throughout this section, the fluctuating Cooper pairs that appear in the electrodes do not aid with transport through the ferromagnetic nanowire initially because of their poor ability to tunnel into it. However, the experimental fact that the wire as long as a micrometer does become superconducting ensures that the pairs eventually are able to tunnel. Sec. III provides a microscopic picture of the Andreev reflection/boundary physics that presumably makes this possible. Therefore, we expect that as the temperature is tuned down to the closest vicinity of the transition, the Cooper pair tunneling takes over the effect of the suppression of the DOS and the upturn in the resistance crosses over to the downturn going through a peak, as observed in experiment.

We notice here in passing that the height of the peak may provide a valuable insight into the competition of the two phenomena and may potentially become a means to measure the boundary spin-orbit coupling that is crucial for the proximity-induced p -wave superconductivity in the wire, the phenomenon of major interest. However, we leave the complicated microscopic theory of spin-orbit-assisted fluctuating pair tunneling for future studies and in this section only extract the leading temperature dependence of this AL type correction. It can be done on the basis of the Ambegaokar-Baratoff formula that

yields⁴¹

$$\delta R_{W/Co}^{(AL)} \propto -\delta(\alpha_R) \int_{-\infty}^{\infty} d\varepsilon \frac{[\delta\nu(\varepsilon)]^2}{\cosh^2\left(\frac{\varepsilon}{2T}\right)}, \quad (67)$$

where $\delta\nu(\varepsilon)$ is the suppression of the DOS obtained in Sec. IV A 2 and we kept a small coefficient $\delta(\alpha_R)$ that includes spin-orbit suppression of the pair-tunneling as obtained in Sec. III.

Note that the integral of the DOS over all energies vanishes identically $\int_{-\infty}^{\infty} d\varepsilon \delta\nu(\varepsilon) = 0$, (the physical interpretation being that the total electron density is conserved and the electrons can only be redistributed across different energies) and a non-zero correction to the resistance in the first order appears only due to the modulating function, $\cosh^{-2}\left(\frac{\varepsilon}{2T}\right)$, and consequently is much weaker (see (66)) than that in the DOS (see (60)). For the pair tunneling, the situation is different as $\int_{-\infty}^{\infty} d\varepsilon \delta\nu^2(\varepsilon)$ is not only non-zero, but is very singular function near the transition. This singularity determines the scaling of the AL correction (67) as

$$\delta R_{W/Co}^{(AL)} \propto -\frac{\delta(\alpha_R)}{(T - T_c)^4}. \quad (68)$$

V. TOPOLOGICAL SUPERCONDUCTIVITY AND MAJORANA FERMIONS

A. Relation to the experiment in Ref. 21

The canonical Kitaev model²⁷, which is the simplest prototype of a one-dimensional topological superconductor, involves one fermion species hopping in a one-dimensional chain and subject to a prescribed p -wave pairing field on the nearest-neighbor bonds. The end points of the chain host single Majorana excitations that are of key interest. One can consider \mathcal{N} replicas of the Kitaev-Majorana model with different p -wave pairing fields for each species but with no mixing between them, i.e. no interband pairing. If \mathcal{N} is even, the end Majoranas are unstable against various perturbations and generally hybridize into relatively uninteresting finite-energy boundary states. In contrast, if \mathcal{N} is odd, the system can then host one Majorana zero-energy state at each end. Recently, theoretical works have addressed a multi-channel generalization of Majorana end states in quasi-one-dimensional structures with Rashba spin-orbit coupling.^{57–60} The works show that the Majorana end states are realized in some parameter regime as long as an odd number of transverse subbands are occupied.

The well-known difficulty in realizing the regime where $(\# \text{ of end Majoranas}) \bmod 2 = 1$ is of course related to the fact that the electrons have spin and consequently come in pairs. Therefore, according to Kitaev²⁷, one necessarily, but not sufficiently, needs to break time-reversal symmetry in the one-dimensional

superconductor to render it topological. The notable and fascinating proposals, where this regime was theoretically shown to be possible, include a heterostructure involving s -wave superconductor/spin-orbit-coupled wire/ferromagnet^{30,39}, a similar heterostructure without a ferromagnet but in a magnetic field^{31,37}, topological insulator/superconductor in a field^{28,40}, and half-metal/superconductor with spin-orbit coupling in the latter³⁸.

If our interpretation of the experimental data in Ref. 21 is correct, we see that this work potentially possesses all necessary ingredients for the realization of the Majorana end states; it has a ferromagnetic crystalline wire in which p -wave superconductivity has been induced. The \mathcal{N} -replica Kitaev-Majorana model discussed here may apply to a thin narrow Co film deposited on top of a three-dimensional W superconductor. The Co film should be highly confined in the direction normal to the Co-W interface so that only one channel is occupied in that direction, and the width of the strip should be smaller than the p -wave coherence length. Since Co is not a half-metal the question is whether a ferromagnetic wire, with both majority and minority carriers, can still host an odd number of end Majorana fermions. This, in principle, may be possible, as what we need is not necessarily to eliminate completely a spin component, but merely to make the two components different from each other such that the total number of occupied subbands is odd, i.e. $(\mathcal{N}_\uparrow + \mathcal{N}_\downarrow) \bmod 2 = 1$. In the simplest model with no inter-subband mixing (considered here), this would imply topological superconductivity. However, we mention that a single-species p -wave superconductor, more akin to the original proposal by Kitaev²⁷, may be possible if the thin film Co wire is replaced by a similar film made of a half-metal such as CrO₂. Notably, experiments have recently shown that CrO₂ can accommodate long-ranged p -wave superconductivity when it is proximity-coupled to a conventional superconductor.²⁰ Majorana bound states should then be realized at the ends of such a half-metal wire when odd number of transverse subbands are occupied.⁵⁷

B. Realizing Majorana end states using a ferromagnetic semiconductor/ferromagnetic superconductor heterostructures

Ref. 21 and the discussion above suggest an even simpler experimental setup for topological superconductivity. Indeed, realizing a one-dimensional topological superconductor using spinful fermions requires lifting the double degeneracy imposed by time-reversal symmetry. In principle, this can be achieved by proximity-inducing a Zeeman gap³⁰ or by applying an external magnetic field^{31,36}. An alternative approach to realizing a one-dimensional topological superconductor is to deposit a ferromagnetic semiconductor wire on top of a ferromagnetic superconductor^{1–4}. A particularly attractive can-

didate ferromagnetic semiconductor is europium oxide (EuO), which is known to possess nearly spin-polarized bands.^{61,62} EuO becomes ferromagnetic below 70K under ambient pressure and the Curie temperature is known to increase with pressure reaching 200K under 1.5×10^5 atmospheres.⁶³ Since its integration with Si and GaN⁶², EuO has garnered much attention for its potential use in spintronic applications. Ferromagnetic superconductors are materials that exhibit intrinsic coexistence of superconductivity and ferromagnetism where the same electrons are believed to be superconducting and ferromagnetic simultaneously. Perhaps the most well-known experimental realizations of ferromagnetic superconductors are the Uranium-based compounds. Following the first experimental realization a decade ago there are now four such compounds¹⁻⁴, two of which exhibit the phenomena at ambient pressures^{2,3}. We propose that depositing URhGe electrodes on the EuO wire, in the arrangement shown in Fig. 1(a), would be conceptually the simplest structure to realize Majorana fermions that would require neither topological insulators nor control over spin-orbit couplings. Application of a magnetic field can further stabilize both the ferromagnetism and superconducting phase.

VI. SUMMARY

In this work, we study temperature-dependent transport properties of a ferromagnetic cobalt nanowire proximity-coupled to superconducting electrodes. The work is largely motivated by a recent experiment,²¹ in which long-ranged superconducting proximity effect was observed in single-crystal Co nanowires coupled to conventional superconductors. We focus particular attention to wires where the transition to superconductivity is preempted by a large and sharp resistance peak near the transition temperature of the electrodes. We explore the possibility of inducing spatially-odd p -wave correlations in the wire via Rashba spin-orbit coupling in the wire-superconductor interface. We then theoretically study the physics of an s -wave-superconductor-ferromagnet tunnel junction in the presence of an interfacial Rashba spin-orbit coupling, and derive an expression for the induced p -wave minigap in terms of the microscopic parameters of the contact.

In the second half of the work, we show how the anomalous resistance peak can be explained within the theory of superconducting fluctuation corrections to conductiv-

ity. In particular, we develop a microscopic theory for the superconducting fluctuation corrections in the tungsten electrodes and discuss how these corrections may lead to corrections in the measured resistance. In the last part of the work, we discuss in detail the possible relevance of the experiment to topological superconductivity and propose a related hybrid system, which provides the simplest physical realization of topological superconductivity and localized Majorana modes.

We note in conclusion that the spin-orbit-assisted proximity-effect scenario considered here is different from the diffusive ferromagnet case, where the likely mechanism for proximity effect is believed to be the odd-frequency pairing.^{22,23} The main argument for the odd-frequency superconductivity is that any anisotropic pairing would decay fast into a disordered metal on a length-scale of order a mean-free-path, while the odd-frequency isotropic pairing is immune from non-magnetic static disorder. This result follows from the Usadel equation if we assume that the non- s -wave part of the disorder-averaged condensate wave-function is small. Then upon linearization of the Usadel equation, further exponential decay of the disorder-averaged p -wave condensate wave-function inevitably follows. We note however that in certain geometries (e.g., if the mean-free path is much larger than the cross-section of the wire, but much smaller than its length), there is no reason to assume that the anisotropic component is small locally near the contacts and consequently the conventional derivation of the Usadel equations from the Eilenberger equations breaks down in these regions. With such assumption about the boundary conditions, the correlator of p -wave condensate wave-functions is not expected to decay exponentially at $T = 0$, in sharp contrast to the exponential decay of the disorder-averaged p -wave condensate wave-function.^{48,64,65} These mesoscopic fluctuation effects will be considered in detail elsewhere.⁶⁶

Acknowledgments

V. G. would like to thank K. Efetov, S. Das Sarma, Y. Oreg, J. Paglione, G. Tkachov and A. Varlamov for discussions. S. T. would like to thank J. Wang for sharing their experimental data, and J. R. Anderson for informative discussions on the cobalt band structure. S. T. would also like thank J. D. Sau for stimulating discussions at an early stage of the work. S. T. was supported by DOE and V. G. by DOE-BES (DESC0001911).

¹ S. S. Saxena, P. Agarwal, K. Ahilan, F. M. Grosche, R. K. W. Haselwimmer, M. J. Steiner, E. Pugh, I. R. Walker, S. R. Julian, P. Monthoux, G. G. Lonzarich, A. Huxley, I. Sheikin, D. Braithwaite and J. Flouquet, *Nature* **406**, 587 (2000).

² D. Aoki, A. Huxley, E. Ressouche, D. Braithwaite, J. Flou-

quet, J.-P. Brison, E. Lhotel and C. Paulsen, *Nature* **413**, 613 (2001).

³ N. T. Huy, A. Gasparini, D. E. de Nijs, Y. Huang, J. C. P. Klaasse, T. Gortenmulder, A. de Visser, A. Hamann, T. Görlach and H. v. Löhneysen, *Phys. Rev. Lett.* **99** 67006 (2007).

- ⁴ T. Akazawa, H. Hidaka, T. Fujiwara, T. C. Kobayashi, E. Yamamoto, Y. Haga, R. Settai and Y. Onuki, J. Phys.: Condens. Matter **16**, L29 (2004).
- ⁵ C. Pfleiderer, M. Uhlarz, S. M. Hayden, R. Vollmer, H. v. Löhneysen, N. R. Bernhoeft and G. G. Lonzarich, Nature **412**, 58 (2001).
- ⁶ L. Bauernfeind, W. Widder and H. Braun, Physica C **254**, 151 (1995).
- ⁷ C. Bernhard, J. L. Tallon, C. Niedermayer, T. Blasius, A. Golnik, E. Brücher, R. K. Kremer, D. R. Noakes, C. E. Stronach and E. J. Ansaldo, Phys. Rev. B **59**, 14099 (1999).
- ⁸ D. J. Pringle, J. L. Tallon, B. G. Walker and H. J. Trodahl, Phys. Rev. B **59**, 11679 (1999).
- ⁹ V. G. Hadjiev, A. Fainstein, P. Etchegoin, H. J. Trodahl, C. Bernhard, M. Cardona and J. L. Tallon, Phys. Stat. Sol. (b) **211**, R5 (1999).
- ¹⁰ S.K.Sinha, G.W.Crabtree, D.G.Hinksand, and H.Mook, Phys. Rev. Lett. **48**, 950 (1982).
- ¹¹ J.W.Lynn, G.Shirane, W. Thomlinson, R.N.Sheltonand, and D.E.Moncton, Phys. Rev. B **24**, 3817 (1981).
- ¹² J.W. Lynn, J.A. Gotaas, R.W. Erwin, R.A. Ferrell, J.K. Bhattacharjee, R.N. Shelton, and P. Klavins, Phys. Rev. Lett. **52**, 133 (1984).
- ¹³ C.-K. Hsu, D. Hsu, C.-M. Wu, C.-Y. Li, C.-H. Hung, C.-H. Lee and W.-H. Li, J. Appl. Phys. **109**, 07B528 (2011).
- ¹⁴ D. A. Dikin, M. Mehta, C. W. Bark, C. M. Folkman, C. B. Eom and V. Chandrasekhar, arXiv:1103.4006v1.
- ¹⁵ J. A. Bert, B. Kalisky, C. Bell, M. Kim, Y. Hikita, H. Y. Hwang and K. A. Moler, Nature Physics **7**, 767 (2011).
- ¹⁶ A. I. Buzdin, Rev. Mod. Phys. **77**, 935 (2005).
- ¹⁷ M. Giroud, H. Courtois, K. Hasselbach, D. Maily and B. Pannetier, Phys. Rev. B **58**, R11872 (1998).
- ¹⁸ V. Petrashov, I. Sosnin, I. Cox, A. Parsons and C. Troadec, Phys. Rev. Lett. **83**, 3281 (1999).
- ¹⁹ V. Pena, Z. Sefrioui, D. Arias, C. Leon, J. Santamaria, M. Varela, S. J. Pennycook and J. L. Martinez, Phys. Rev. B **69**, 224502 (2004).
- ²⁰ R. S. Keizer, S. T. B. Goennenwein, T. M. Klapwijk, G. Miao, G. Xiao and A. Gupta, Nature **439**, 825 (2006).
- ²¹ J. Wang, M. Singh, M. Tian, N. Kumar, B. Liu, C. Shi, J. K. Jain, N. Samarth, T. E. Mallouk and M. H. W. Chan, Nature Physics **6**, 389 (2010).
- ²² F. S. Bergeret, A. F. Volkov and K. B. Efetov, Rev. Mod. Phys. **77**, 1321 (2005).
- ²³ F. S. Bergeret, A. F. Volkov and K. B. Efetov, Phys. Rev. Lett. **86**, 4096 (2001).
- ²⁴ V. L. Berezinskii, JETP Lett. **20**, 287 (1974).
- ²⁵ M. Eschrig, J. Kopu, J. C. Cuevas and G. Schön, Phys. Rev. Lett. **90**, 137003 (2003).
- ²⁶ M. Eschrig and T. Löfwander, Nature Physics **4**, 138 (2008).
- ²⁷ A. Yu. Kitaev, Phys.-Usp. **44**, 131 (2001).
- ²⁸ L. Fu and C. L. Kane, Phys. Rev. Lett. **100**, 096407 (2008).
- ²⁹ Y. Tanaka, T. Yokoyama, and N. Nagaosa, Phys. Rev. Lett. **103**, 107002 (2009).
- ³⁰ J. D. Sau, R. M. Lutchyn, S. Tewari and S. Das Sarma, Phys. Rev. Lett. **104**, 040502 (2010).
- ³¹ R. M. Lutchyn, J. D. Sau and S. Das Sarma, Phys. Rev. Lett. **105**, 077001 (2010).
- ³² Y. Oreg, G. Refael and F. v. Oppen, Phys. Rev. Lett. **105**, 177002 (2010).
- ³³ V. Shivamoggi, G. Refael and J. E. Moore, Phys. Rev. B **82**, 041405(R) (2010).
- ³⁴ P. A. Ioselevich and M. V. Feigel'man, Phys. Rev. Lett. **106**, 077003 (2011).
- ³⁵ S. B. Chung, H.-J. Zhang, X.-L. Qi, S.-C. Zhang, Phys. Rev. B **84**, 060510 (2011).
- ³⁶ P. A. Lee, arXiv:0907.2681.
- ³⁷ J. Alicea, Phys. Rev. B **81**, 125318 (2010).
- ³⁸ M. Duckheim and P. Brouwer, Phys. Rev. B **83**, 054513 (2011).
- ³⁹ S. Tewari, J. D. Sau and S. Das Sarma, Ann. Phys. (NY) **325**, 219 (2010).
- ⁴⁰ A. Cook and M. Franz, Phys. Rev. B **84**, 201105(R) (2011).
- ⁴¹ A. I. Larkin and A. A.Varlamov, In *Superconductivity: Conventional and Unconventional Superconductors*, ed. K. H. Bennemann and J. B. Ketterson, (Springer, Berlin, 2004), Ch. 10, p. 369.
- ⁴² A. A.Varlamov, G. Balestrino, E. Milani and D. V. Livanov, Adv. Phys. **48**, 655 (1999).
- ⁴³ J. R. Anderson and J. E. Schirber, J. Appl. Phys. **52**, 1630 (1981).
- ⁴⁴ F. Batallan, I. Rosenman and C. B. Sommers, Phys. Rev. B **11**, 545 (1975).
- ⁴⁵ C. M. Singal and T. P. Das, Phys. Rev. B **16**, 5068 (1977).
- ⁴⁶ G. J. McMullan, D. D. Pilgram and A. Marshall, Phys. Rev. B **46**, 3789 (1992).
- ⁴⁷ J. W. A. Robinson, S. Piano, G. Burnell, C. Bell and M. G. Blamire, Phys. Rev. Lett. **97**, 177003 (2006).
- ⁴⁸ F. Zhou and B. Spivak, cond-mat/9906177v3.
- ⁴⁹ A. F. Volkov, P. H. C. Magnee, B. J. van Wees and T. M. Klapwijk, Physica C **242**, 261 (1995).
- ⁵⁰ G. Tkachov, Physica C **417**, 127 (2005).
- ⁵¹ L. B. Ioffe, A. I. Larkin, A. A. Varlamov and L.Yu, Phys. Rev. B **47**, 8936 (1993).
- ⁵² G. Balestrino, M. Marinelli, E. Milani, A. A. Varlamov and L. Yu, Phys. Rev. B **47**, 6037 (1993).
- ⁵³ G. Balestrino, E. Milani and A. A. Varlamov, Physica C **210**, 386 (1993).
- ⁵⁴ V. M. Galitski and A. I. Larkin, Phys. Rev. B **63**, 174506 (2001).
- ⁵⁵ I. S. Beloborodov, K. B. Efetov, A. V. Lopatin, V. M. Vinokur, Rev. Mod. Phys. **79**, 469 (2007).
- ⁵⁶ C. Di Castro, R. Raimondi, C. Castellani, and A. A. Varlamov, Phys. Rev. B **42**, 10211 (1990).
- ⁵⁷ A. C. Potter and P. A. Lee, Phys. Rev. Lett. **105**, 227003 (2010).
- ⁵⁸ A. C. Potter and P. A. Lee, Phys. Rev. B **83**, 094525 (2011).
- ⁵⁹ R. M. Lutchyn, T. D. Stanescu and S. Das Sarma, Phys. Rev. Lett. **106**, 127001 (2011).
- ⁶⁰ T. D. Stanescu, R. M. Lutchyn and S. Das Sarma, Phys. Rev. B **84**, 144522 (2011).
- ⁶¹ P. G. Steeneken, L. H. Tjeng, I. Elfimov, G. A. Sawatzky, G. Ghiringhelli, N. B. Brookes and D.-J. Huang, Phys. Rev. Lett. **88**, 047201 (2002).
- ⁶² A. Schmehl, V. Vaithyanathan, A. Herrnberger, S. Thiel, C. Richter, M. Liberati, T. Heeg, M. Röckerath, L. F. Kourkoutis, S. Mühlbauer, P. Böni, D. A. Muller, Y. Barash, J. Schubert, Y. Idzerda, J. Mannhart and D. G. Schlom, Nature Mater. **6**, 882 (2007).
- ⁶³ N. M. Souza-Neto, D. Haskel, Y.-C. Tseng and G. Laperot, Phys. Rev. Lett. **102**, 057206 (2009).
- ⁶⁴ F. Zhou and B. Spivak, Phys. Rev. Lett. **80**, 5647 (1998).
- ⁶⁵ V. M. Galitski and A. I. Larkin, Phys. Rev. Lett. **87**, 087001 (2001).
- ⁶⁶ S. Takei and V. Galitski, to be published.